The Eurasia Proceedings of Science, Technology, Engineering & Mathematics (EPSTEM)
ISSN: 2602-3199

The Eurasia Proceedings of Science, Technology, Engineering & Mathematics (EPSTEM), 2023

Volume 26, Pages 183-189

IConTES 2023: International Conference on Technology, Engineering and Science

TRIAC Based Isolated AC Load Drive Equivalent Circuit Design of Solid-State Relay

Gonca Uslu - Ozkucuk
OSTIM Technical University

Abstract: Electronic main boards generally provide the supply and control functions of a system. All electronic main boards include inputs and outputs and are designed according to the design requirements. In this study, a safe and low-cost switching mode power supply (SMPS) board is designed using a flyback converter topology to drive the AC and DC outputs. The triode for alternating current (TRIAC)-based safe and low-cost main board includes a flyback configured transformer with additional winding for driving the TRIAC as an AC output switch in noise immune quadrants II and III. TRIAC is used to switch AC outputs instead of a relay, and the isolation distances of the safety criteria are provided by an optocoupler. In this way, the relay usage is over, and one TRIAC and one optocoupler do the same work that is done by one relay. In this way, the cost of the AC output switch decreases. In addition, the number of AC switches covering the area on the printed-circuit board (PCB) of the mainboard decreases. The flyback topology is designed with half-wave rectified and the transformer is designed with extra winding for producing negative voltage with respect to primer reference for providing negative gate current of TRIAC. TRIAC-based AC output switched, safe, and low-cost main boards can be used for white good main boards, automation (PLC) applications, and automotive electronic control systems. This study provides cost-effective solutions in these areas.

Keywords: TRIAC, Flyback converter, Power electronic, Circuit design

Introduction

Main boards are used in almost every moment of our lives. Most electronic devices include a mainboard with a converter topology, which has different capacities from µW levels to MW. Middle- and high-segment power converters and mainboards are generally used for energy systems, especially in renewable areas such as solar and wind or hybrid applications (Bayrak, 2015; Bayrak & Kabalci, 2016).

The flyback topology is a highly preferred SMPS topology for most mainboards because of its simple, isolated, and efficient structure. There are important design works on flyback topology in the literature. Generally, studies on isolated flyback topology focus on different aims. When we study the literature from the main board design perspective of an isolated flyback converter, we can see the classical topology and traditional methods in the constructions. Most of the designs include an input section of DC or AC type with full wave rectifier bridge diode and filter block, isolated flyback transformer according to needs, switching element and feedback section from seconder side (with an opto-coupler) or primer side regulation (Chang & Chen, 2013; Coruh et al., 2010; Reshma et al., 2016). Multiple DC output designs are commonly used and are more suitable for a main board design because all DC voltage levels (3.3 V, 5 V, 7.2 V, 12 V, etc.) for driving the microcontroller and other auxiliary elements in the main board are produced in multiple output designs (Hashjin, 2017; Myderrizi & Ozbey, 2014). When we examine the literature on AC TRIAC switches with flyback, we find much work on TRIAC dimming flyback converters for led driver applications. These systems include a controlled TRIAC dimmer on the input line to obtain smooth brightness (Moon et al., 2014; Zhang et al., 2012). These systems are related to the control of the driver, but our design TRIAC usage aim is related to safe AC output switching They are completely different applications. Our main idea is to integrate a TRIAC as an AC output switch to a flyback topology, which is modified to drive the TRIAC in noise immune quadrants II and III in a mainboard frame (*Fundamental Characteristics of Thyristors*).

In this study, we designed a main board that can be used for daily life electronic devices such as whitegoods, small household appliances, automation, and automotive main boards. Our system works with a one-phase AC mains source input or can be modified with respect to a DC source input for automotive applications. The designed system includes a modified flyback topology for driving AC outputs with a TRIAC and provides the isolation of primer–seconder distance safety criteria. The power capacity of the system is determined up to 10W. This means that, designed mainboard can drive DC outputs up to nearly 8 W from the seconder winding and up to nearly 10 (ten) TRIACs from the extra TRIAC drive winding for 10 AC outputs. This main board topology can be integrated in all white goods and small household appliances, or it can be used as a mainboard for a middle segment automation system.

Design Specifications

Determining the design specification of the system is a critical step because theoretical calculations of the design are performed according to these specifications. In this system, a 10 W output power flyback converter is designed. The designed mainboard can drive DC outputs up to 8 W from a seconder winding and up to 10 (ten) TRIACs (with 20 mA gate current) from extra TRIAC drive winding for 10 AC outputs. The system specifications are described in Table 1.

Table 1. System specification table

System specification	Value
Min. and Max. input voltage	$V_{line,min}$: 170V $V_{line,max}$: 265V
Input voltage frequency	f_L: 50Hz
Max. output power	10W
Design efficiency	0.85

The designer determined these specifications according to the project needs. This board is designed for European grid AC mains with 220–230 V, 50 Hz, and system immunity of AC mains tolerances are determined as 25%; therefore, maximum and minimum input voltages are determined with respect to this consideration. In addition, the design includes an extra winding to produce negative voltage with respect to the primer Notr line. In this way, we can obtain DC and AC outputs that are driven by a TRIAC with a negative gate current. TRIAC driving is performed by a control signal that triggers the TRIAC gate with respect to zero cross moments using an optocoupler. TRIAC driving circuit is shown in Figure 1.

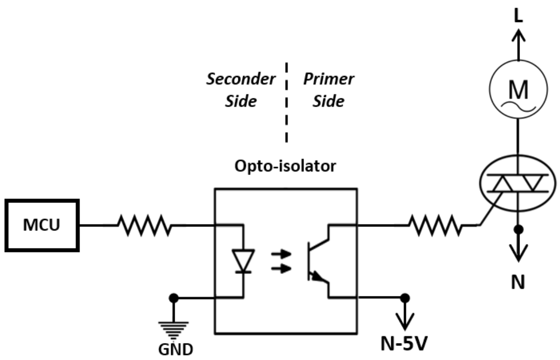

Figure 1. TRIAC driving schematic

Theoretical Analysis and Design

The flyback topology contains important basic elements. They are input capacitance (bulk capacitance), switching element, transformer primer-seconder inductance, output diode, and output capacitance. The important problem in the design work is determining these elements and the extra TRIAC winding circuit. In this section, the theoretical values of these important elements and other design parameters of the system are calculated with respect to the formulas given below (Hart, 2010; Rashid, 2011). The system general block diagram is shown in Figure 2.

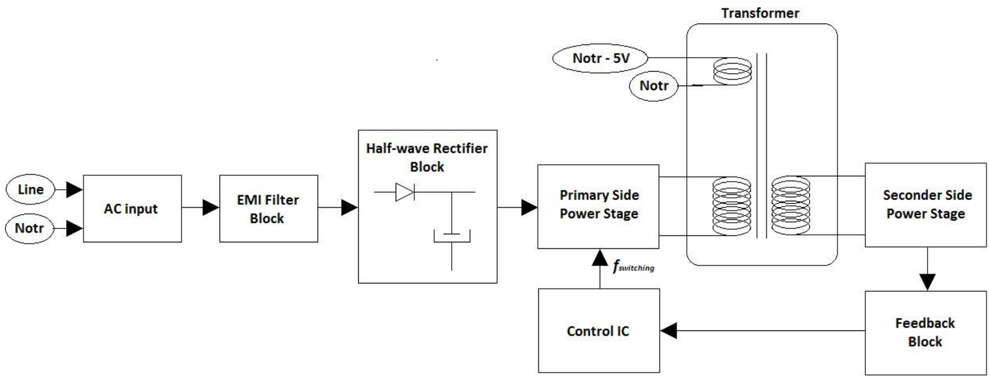

Figure 2. Block schematic of proposed design

Input capacitance is an important energy storage element in the design. Therefore, first maximum and minimum DC voltages on the capacitor and input power must be determined. Generally, European grid AC mains with 220–230 V, 50 Hz system uses 1 uF per watt. This generalisation comes from 50 Hz sinus waveform rectifying. In our design, we use a half-wave rectifier because of the usage of Notr as primer ground. If we want a DC voltage from 50 Hz sinus wave, we must keep the DC link voltage ripple at a certain value. This value is related to the ripple time and one-period time ratio (Dch). Generally, this ratio is selected as 0.2 or 0.25 (Hart, 2010; Rashid, 2011). If it is greater than 0.25, the system discharge time is larger and the energy of the primer does not compensate for the seconder.

The input power is shown in Equation (1):

$$Po = \frac{P_{in}}{Eff} \tag{1}$$

The minimum and maximum DC voltages on the capacitor are given by Equations (2) and (3), respectively:

$$2V_{DC_{min}} = \sqrt{2\left(V_{line_{min}}\right)^2 - \frac{P_{in}(1 - D_{ch})}{C_{bulk} f_L}} \tag{2}$$

$$2V_{DC_{max}} = \sqrt{2} V_{line_{max}} \tag{3}$$

The switching element is a metal oxide semiconductor field effect transistor (MOSFET). The selection of the MOSFET depends on the drain–source voltage capacity. The voltage drop on the drain-source of the MOSFET depends on maximum DC voltage on the primer capacitor plus the reflected voltage from the seconder side to the primer side. The maximum duty cycle of the MOSFET is determined by the relationship between the minimum primer DC voltage and the reflected voltage. The maximum duty cycle (D_{max}) must be selected intelligently. If D_{max} is selected as a small value, the stress on the switching MOSFET decreases but the stress on the output diode increases. Therefore, there is a trade-off between D_{max} and stress on the MOSFET and output diode. In our design, we selected the maximum duty cycle of the MOSFET as 0.33. This value provides the optimum stress on the MOSFET and output diode.

The reflected voltage is shown in Equation (4):

$$\mathrm{V_{Reflected}} = \frac{\mathrm{D_{max}}}{1 - \mathrm{D_{max}}} \mathrm{V_{DC_{min}}} \tag{4}$$

MOSFET drain-source nominal voltage is shown in Equation (5):

$$V_{DS_{nom}} = V_{DC_{max}} + V_{Reflected} \tag{5}$$

Transformer primer inductance is another important parameter in the design. The flyback converter can operate in discontinuous conduction mode (DCM) and continuous conduction mode (CCM) according to the input voltage level and load condition. The worst case for both the DCM and CCM working modes is full load with a minimum input voltage. Primer inductance calculations were performed in accordance with this consideration.

Primer inductance is shown in Equation (6):

$$L_{primer} = \frac{\left(V_{DC_{min}} D_{max}\right)^2}{2 P_{in} f_{sw}} \tag{6}$$

After this stage MOSFET current capacity is determined with respect to calculated primer inductance value.

Nominal MOSFET drain-source current is shown in Equation (7):

$$I_{nominal} = \frac{P_{in}}{V_{DC_{min}} D_{max}} \tag{7}$$

Primer current ripple is shown in Equation (8):

$$\Delta I = \frac{V_{DC_{min}} D_{max}}{L_{primer}\, f_{sw}} \tag{8}$$

Maximum MOSFET drain-source current is shown in Equation (9):

$$I_{DS_{peak}} = I_{nominal} + \frac{\Delta I}{2} \tag{9}$$

Seconder inductance of the transformer is determined by the winding turns ratio because the input and output voltages are directly proportional to the winding ratio. In addition, the transformer core type, dimensions, output power level, and frequency are another factor for seconder inductance. In this design, we selected seconder inductance and extra Notr-5V winding inductance as 30 (thirty) times smaller than the primer inductance because the system works at 220 V and 50 Hz under optimum conditions. Thus, the primer DC voltage is equal to 154V, as shown in Equation (3), under this condition. The seconder voltage was 5 V, and the ratio between the primer and seconder was nearly 30. This value provides the work of the system effectively. The selection of the output diode depends on the nominal current and reverse voltage of the diode. The output diode is selected with respect to these considerations.

Nominal current value of output diode is shown in Equation (10):

$$I_{out_{nom}} = I_{DS} \sqrt{\frac{1 - D_{max}}{D_{max}} \frac{V_{reflected}}{V_{out} + V_{f_{diode}}}} \tag{10}$$

Maximum reverse voltage on the output diode is shown in Equation (11):

$$V_{D_{nom}} = V_{out} + \frac{V_{DC_{max}}\left(V_{out} + V_{f_{diode}}\right)}{V_{reflected}} \tag{11}$$

These calculations show the limit values of the output diode selection. The selection of the diode must be performed with margins for a reliable design. If the output diode is selected with current and reverse voltage smaller than the theoretical results, design does not work reliable. The output capacitor is another important element in the design and depends on the ripple current of the output.

Output capacitor ripple current is shown in Equation (12):

$$I_{cap} = \sqrt{{I_{out_{nom}}}^2 - {I_{average}}^2} \tag{12}$$

The calculated capacitor ripple current must be smaller than the selected capacitor ripple currents All calculations and selected components with margins for reliable design values are listed in Table 2.

Table 2. Theoretical analysis results table

Parameters	Theoretical Values	Selected Values
V_{DCmin}	120.2V	-
V_{DCmax}	187.3V	-
C_{bulk}	11.76uF	12uF, 400V
V_{DSnom}	247.4V	250V
I_{DSpeak}	0.606A	3.5A
L_{primer}	186.6uH	200u
$L_{seconder}$	6.05uH	7u
$L_{extra\_winding}$	6.05uH	7u
I_{outnom}, V_{Dnom}	4.56A, 22.54V	6A, 60V
I_{cap}, $C_{seconder}$	4.09A	300uF, 6.3V

Simulation Results

The proposed design is simulated in the LT Spice simulation program with respect to the calculated and selected values in the theoretical analysis and design section. The system contains a flyback converter with a feedback line from the seconder and a 5 V, 2 A DC output. In addition, the system is designed to be completely safe, which means that there is no electrically conductive element between the primer and seconder. Extra TRIAC driving winding produces nearly negative 5 V according to the primer ground (Notr). The LT spice circuit schematic is shown in Figure 3.

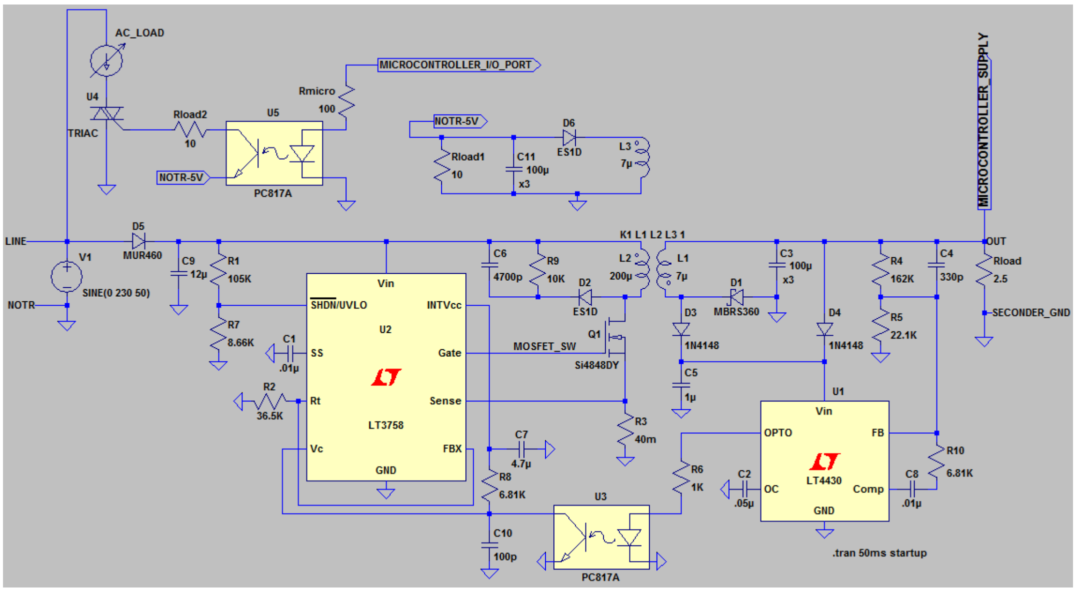

Figure 3. LT Spice designed circuit

In this section, the designed LT Spice circuit is run and the obtained results are interpreted. In the simulations, LT components are mostly used, and the parameters of the components are reset according to Table. 2. The feedback of the system is taken by a seconder DC output of 5 V, and the switching frequency of the SMPS IC is 350 kHz.

The simulation time of the design is 50 ms. A seconder DC output 5 V, 2 A, and extra TRIAC winding Notr-5V is obtained successfully in Figure 4. When we examine Fig. 4, with a second DC output of 5 V, the stability of the system is observed at 4th msec. Seconder DC output 5 V is obtained exactly 5 V but primer extra TRIAC winding Notr-5V is obtained nearly negative value -5V certain negative value is -4.70V because feedback is taken from seconder side DC output 5V. We can obtain 10 W DC output power for DC loads and 2.35W for TRIAC gate driving for AC loads. This system can drive five TRIACs with a gate current of 50 mA. The number of TRIACs can be increased if a low gate current-triggered TRIAC is preferred.

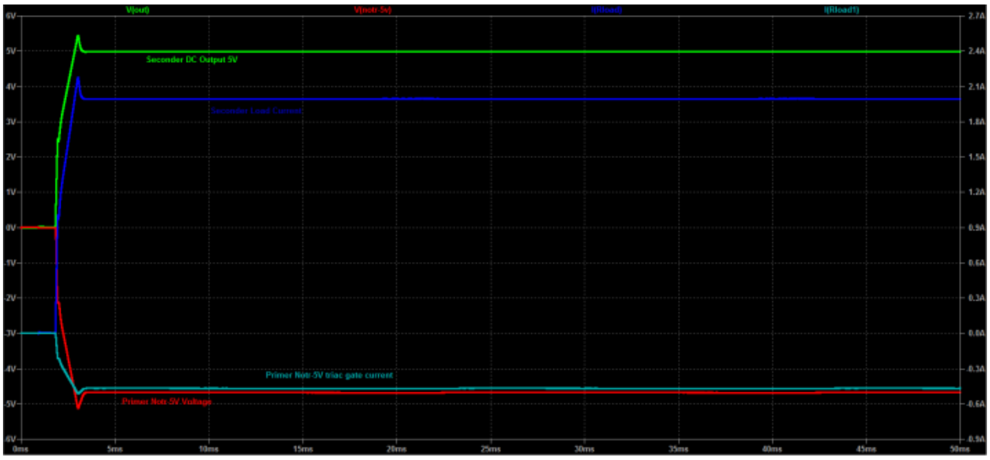

Figure 4. DC output 5 V and extra winding Notr-5V with currents under full load

The system input is 230 V, 50 Hz AC, and a half-wave rectifier is used to obtain the DC bulk capacitor voltage. The input values are shown in Fig. 5. When we examine Fig. 5, 12uF bulk capacitor is sufficient for obtaining DC voltage from the half-wave rectifier block. The system works in the DCM mode, and the inrush current is at acceptable levels according to the input diode. The design works under less stress and is stable.

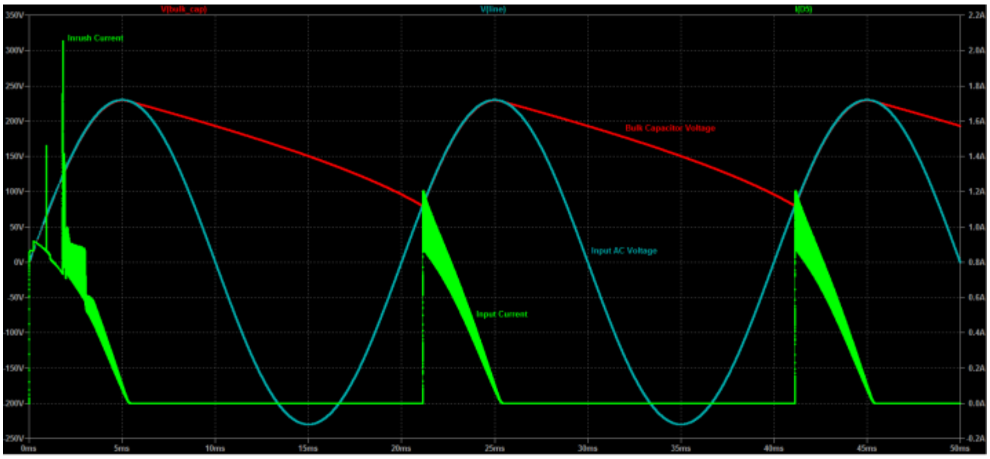

Figure 5. AC input, bulk capacitance voltage, and input current

Conclusion

In this study, we have two main advantages over the traditional main board design with flyback topology. We eliminated relay usage for AC loads in the main boards. One TRIAC and one optocoupler with the help of an extra TRIAC winding do the same work by providing safety criteria instead of relay. In this way, the cost of the system decreases and the PCB design is more compact and smaller than the traditional design. The energy consumption of one relay is greater than that of one TRIAC. If we consider more than one AC output system, the energy consumption decreases in our new design topology.

Scientific Ethics Declaration

The author declares that the scientific ethical and legal responsibility of this article published in EPSTEM journal belongs to the author.

Acknowledgements or Notes

* This article was presented as an oral presentation at the International Conference on Technology, Engineering and Science (www.icontes.net) held in Antalya/Turkey on November 16-19, 2023.

References

Bayrak, G. (2015). A remote islanding detection and control strategy for photovoltaic-based distributed generation systems. *Energy Conversion and Management*, *96*, 228-241.

Bayrak, G., & Kabalci, E. (2016). Implementation of a new remote islanding detection method for wind–solar hybrid power plants. *Renewable and Sustainable Energy Reviews*, *58*, 1-15.

Chang, C.J. , & Chen, C. L. (2013). An isolated output-feedback scheme with minimized standby power for SMPS. *IEEE Transactions on Power Electronics*, *28*(11), 5140-5146.

Coruh, N., Urgun, S., & Erfidan, T. (2010). Design and implementation of flyback converters. 2010 5*th IEEE conference on industrial electronics and applications, Fundamental Characteristics of Thyristors*. Retrieved from http://www.littelfuse.com.

Hart, D. W. (2010). *Power electronics*. McGraw-Hill.

Hashjin, S. A. (2017). *Cok cıkıslı yalıtılmıs flyback donusturucu tasarımı ve uygulaması.* (Master'thesis) Gazi University, Ankara, Turkey.

Moon, S., Koo, G.-B., & Moon, G.-W. (2014). Dimming-feedback control method for TRIAC dimmable LED drivers. *IEEE Transactions on industrial Electronics*, *62*(2), 960-965.

Myderrizi, I., & Ozbey, E. (2014). A low power multiple output switch-mode power supply with wide input range. *Analog Integrated Circuits and Signal Processing*, *81*, 431-441.

Rashid, M. H. (2011). *Power electronics handbook, Devices, circuits and applications* .(3rd ed.). Elsevier.

Reshma, K., Sreenath, R., & Pai, N. (2016). Design and implementation of an isolated switched-mode power supply for led application. *International Conference on Computation of Power, Energy Information and Commuincation (ICCPEIC)*

Zhang, J., Zeng, H., & Jiang, T. (2012). A primary-side control scheme for high-power-factor LED driver with TRIAC dimming capability. *IEEE transactions on power electronics*, *27*(11), 4619-4629.

Author Information

Gonca Uslu-Ozkucuk
OSTIM Technical University, Vocational School of Higher Education, Department of Electricity and Energy, Electricity Program, Ankara, Turkey
Ostim, 100. Yıl Blv., 55/F, 06374
Ostim Osb/Yenimahalle/Ankara, Turkey
Contact e-mail: *gonca.usluozkucuk@ostimteknik.edu.tr*

To cite this article:

Uslu-Ozkucuk, G. (2023). TRIAC based isolated AC load drive equivalent circuit design of solid-state relay. *The Eurasia Proceedings of Science, Technology, Engineering & Mathematics (EPSTEM), 26,* 183-189.